Ramaiah, A. (1974) *Curr. Top. Cell. Regul. 8*, 297–345.
Rose, I. A. (1971) *Exp. Eye Res. 11*, 264–272.
Salas, M. L., Vinuela, Salas, M., & Sols, A. (1965) *Biochem. Biophys. Res. Commun. 19*, 371–376.
Salhany, J. M., Yamane, T., Shulman, R. G., & Ogawa, S. (1975) *Proc. Natl. Acad. Sci. U.S.A. 72*, 4966–4970.
Serrano, R., & DelaFuente, G. (1974) *Mol. Cell. Biochem. 5*, 161–171.
Sols, A. (1967) in *Aspects of Yeast Metabolism* (Mills, A. K., & Krebs, H. A., Eds.) pp 47–66, Blackwell Scientific Publications, Oxford.
Sols, A. (1976) in *Reflections on Biochemistry* (Kornberg, A., Horecker, B. L., Cornudella, L., & Oro, J., Eds.) pp 199–206, Pergamon Press, Oxford.
Sols, A. (1981) *Curr. Top. Cell. Regul. 19*, 77–101.
Sols, A., Grancedo, C., & DelaFuente, G. (1971) in *The Yeasts* (Rose, A. H., & Harrison, J. S., Eds.) Vol. 2, pp 271–307, Academic Press, London.
Stellwagen, E., & Wilgus, H. (1975) *Methods Enzymol. 42*, 78–85.
Su, S., & Russell, P. J. (1968) *J. Biol. Chem. 243*, 3826–3833.
Tejwani, G. A. (1978) *Trends Biochem. Sci. 3*, 30–33.
Vinuela, E., Salas, M. L., & Sols, A. (1963) *Biochem. Biophys. Res. Commun. 12*, 140–145.

Protonation Mechanism and Location of Rate-Determining Steps for the *Ascaris suum* Nicotinamide Adenine Dinucleotide–Malic Enzyme Reaction from Isotope Effects and pH Studies†

Dennis M. Kiick, Ben G. Harris, and Paul F. Cook*
Department of Biochemistry, North Texas State University/Texas College of Osteopathic Medicine, Denton, Texas 76203
Received June 24, 1985

ABSTRACT: The pH dependence of the kinetic parameters and the primary deuterium isotope effects with nicotinamide adenine dinucleotide (NAD) and also thionicotinamide adenine dinucleotide (thio-NAD) as the nucleotide substrates were determined in order to obtain information about the chemical mechanism and location of rate-determining steps for the *Ascaris suum* NAD–malic enzyme reaction. The maximum velocity with thio-NAD as the nucleotide is pH-independent from pH 4.2 to 9.6, while with NAD, V decreases below a pK of 4.8. V/K for both nucleotides decreases below a pK of 5.6 and above a pK of 8.9. Both the tartronate pK_i and V/K_{malate} decrease below a pK of 4.8 and above a pK of 8.9. Oxalate is competitive vs. malate above pH 7 and noncompetitive below pH 7 with NAD as the nucleotide. The oxalate K_{is} increases from a constant value above a pK of 4.9 to another constant value above a pK of 6.7. The oxalate K_{ii} also increases above a pK of 4.9, and this inhibition is enhanced by NADH. In the presence of thio-NAD the inhibition by oxalate is competitive vs. malate below pH 7. For thio-NAD, both ^DV and $^D(V/K)$ are pH-independent and equal to 1.7. With NAD as the nucleotide, ^DV decreases to 1.0 below a pK of 4.9, while $^D(V/K_{NAD})$ and $^D(V/K_{malate})$ are pH-independent. Above pH 7 the isotope effects on V and the V/K values for NAD and malate are equal to 1.45, the pH-independent value of ^DV above pH 7. From the above data, the following conclusions can be made concerning the mechanism for this enzyme. Substrates bind to only the correctly protonated form of the enzyme. Two enzyme groups are necessary for binding of substrates and catalysis. Both NAD and malate are released from the Michaelis complex at equal rates which are equal to the rate of NADH release from E–NADH above pH 7. Below pH 7 NADH release becomes more rate-determining as the pH decreases until at pH 4.0 it completely limits the overall rate of the reaction.

The NAD[1]–malic enzyme from *Ascaris suum*, isocitrate dehydrogenase, and NADP–malic enzyme from pigeon liver all catalyze the same type of reaction, a divalent metal dependent oxidative decarboxylation utilizing NAD(P) as the electron acceptor. However, the enzymes listed above are quite different with respect to their kinetic properties. The pigeon liver enzyme has an ordered kinetic mechanism (Hsu & Lardy, 1967; Schimerlik & Cleland, 1977a), while both ICDH[1] (Uhr et al., 1974) and the ascarid enzyme (Park et al., 1984) have random mechanisms. Further, release of reduced nucleotide completely limits the maximum rate for both ICDH (Uhr et al., 1974) and the pigeon liver enzyme (Schimerlik & Cleland,

† This research was supported by National Institutes of Health Grants AI-12331 (to B.G.H.) and GM-31686 (to P.F.C.), Grant BRSG S07 RR07195-03 (to P.F.C.) awarded by the Biomedical Research Grant Program, Division of Research Resources, National Institutes of Health, and Grants B-997 (to B.G.H.) and B-1031 (to P.F.C.) from the Robert A. Welch Foundation. P.F.C. is the recipient of NIH Research Career Development Award AM-01155.

[1] Abbreviations: BTP, [bis(2-hydroxyethyl)amino]tris(hydroxymethyl)propane; Caps, 3-(cyclohexylamino)propanesulfonic acid; Ches, 2-(cyclohexylamino)ethanesulfonic acid; DTT, dithiothreitol; EDTA, ethylenediaminetetraacetic acid; EPR, electron paramagnetic resonance; Hepes, *N*-(2-hydroxyethyl)piperazine-*N*′-2-ethanesulfonic acid; ICDH, NADP–isocitrate dehydrogenase; Mes, 2-(*N*-morpholino)ethanesulfonic acid; NAD, nicotinamide adenine dinucleotide; NADP, nicotinamide adenine dinucleotide phosphate; Ox, oxalate; PAGE, polyacrylamide gel electrophoresis; Pipes, 1,4-piperazinediethanesulfonic acid; SDS, sodium dodecyl sulfate; Taps, 3-[[tris(hydroxymethyl)methyl]amino]propanesulfonic acid.

0006-2960/86/0425-0227$01.50/0

1977a) at neutral pH, while prior to this study, information on the rate-limiting steps for the NAD–malic enzyme was unknown.

Recently, Cook & Cleland (1981a,b,c) have shown that information on the mechanism of protonation and also the chemical mechanism for the enzyme being studied can be obtained from the pH dependence of the kinetic parameters and primary isotope effects on V and V/K for substrates. Of the three enzyme systems discussed above, this has been accomplished for only ICDH and the pigeon liver enzyme. Since the maximum velocities for ICDH (Cook & Cleland, 1981b) and the pigeon liver enzyme (Schimerlik & Cleland, 1977a) are pH-dependent, substrates bind to both the protonated and unprotonated forms of the enzyme, but only the unprotonated Michaelis complex is catalytically competent. Further, the pH variation of ^{D}V and $^{D}(V/K_{malate})$ for the pigeon liver enzyme indicates that malate is not sticky,[2] while for ICDH, isocitrate is sticky (Cook & Cleland, 1981a).

This study presents a detailed investigation of the pH dependence of the steady-state kinetic parameters and K_i values for competitive inhibitors, as well as kinetic data for the pH dependence of V and V/K for thio-NAD for the ascarid NAD–malic enzyme. In addition, the pH variation of the primary deuterium isotope effects has been obtained with both NAD and thio-NAD as the nucleotide. These data further confirm the randomness of the kinetic mechanism proposed by Park et al. (1984) and provide information on the location of rate-determining steps for this reaction. Moreover, the data suggest that two enzyme residues are necessary for catalysis. Protonation and chemical mechanisms consistent with the data are proposed for the *Ascaris suum* NAD–malic enzyme.

Materials and Methods

Chemicals and Enzymes. Mitochondrial NAD–malic enzyme from *Ascaris suum* was purified according to the procedure of Allen & Harris (1981). The enzyme had a final specific activity of 40 units/mg. The compounds L-malate, thio-NAD, and dithiothreitol were from Sigma. NAD and NADH were purchased from Boehringer-Mannheim. Ethanol-d_6 (99 atom % D) was from Merck. L-Malate-2-*d* was prepared according to the method of Viola et al. (1979). All other reagents and chemicals were obtained from commercially available sources and were of the highest quality available.

Metal Chelate Correction. Since metal–ligand chelate complexes are not reactants for the NAD–malic enzyme reaction, the concentration of reactants and inhibitors added to the reaction mixture had to be corrected for the concentration of metal–ligand chelate complex (Park et al., 1984). The following dissociation constants were used in the calculations: Mg–malate, 25.1 mM; Mg–NAD, 19.5 mM; Mg–Mes, 160 mM; Mg–tartronate, 6.8 mM; Mg–oxalate, 1.7 mM; Mg–2Ox, 58.0 mM[2] (Martell & Smith, 1977; Dawson et al., 1969; Good et al., 1966). The dissociation constant for Mg–thio-NAD was assumed to be the same as that for Mg–NAD.

At pH values less than 5, additional correction was necessary in order to take into account the concentration of protonated metal–ligand chelate complex. This was accomplished by utilizing the Henderson–Hasselbach equation to calculate the concentrations of protonated and unprotonated ligand present at the pH at which the assay was to be run and then using equations described by Park et al. (1984) to calculate the concentrations of protonated and unprotonated metal–ligand chelate complex present for a given concentration of free uncomplexed ligand. Additional dissociation constants used to perform the above calculation are as follows: Mg–hydrogen malate, 150 mM, pK of 4.7; Mg–hydrogen tartronate, 58.9 mM, pK of 4.2 (Martell & Smith, 1977). All other reaction components gave negligible corrections under the conditions used.

Substrate Calibration. The precision of V/K isotope effects measured by the direct comparison technique requires that one accurately know the concentrations of labeled and unlabeled substrates (Cleland, 1982). Therefore, all substrate concentrations were calibrated enzymatically by end-point analysis as described by Cook et al. (1980). Concentrations of deuterium-labeled or unlabeled L-malate were determined by using 2 units of chicken liver malic enzyme in 100 mM Taps, pH 9.0. All assays contained the following: NADP, 1 mM; $MgSO_4$, 2 mM; and DTT, 0.2 mM. Solutions of NAD were calibrated with *Ascaris suum* malic enzyme and excess malate ($20K_m$) and $MgSO_4$ ($20K_i$) in 100 mM Taps, pH 9.0, and 1.0 mM DTT. The concentrations from several determinations were in agreement within 1%.

Initial Velocity Studies. Malic enzyme was assayed spectrophotometrically in the direction of oxidative decarboxylation on a Gilford 250 spectrophotometer, using a Brinkman Servogor 210 chart recorder with multispeed drive. Full-scale sensitivities of 0.05, 0.1, and 0.2 OD and chart speeds in the range of 0.5–12 cm/min were used. All assays were carried out at 25 °C. The temperature was maintained with a circulating water bath with the capacity to heat and cool the thermospacers of the Gilford. Reaction cuvettes were 1 cm in path length and 1 or 3 mL in volume. All cuvettes were incubated for at least 10 min in the water bath and 5 min in the cell compartment prior to initiation of the reaction. Assay temperatures were routinely monitored with a YSI telethermometer while the cuvette was still in the cell compartment. A typical assay contained 100 mM buffer (see pH Studies), 1 mM DTT, variable concentrations of divalent metal, malate, and NAD, and 8.4 nM malic enzyme. The reaction was started by the addition of enzyme, and the production of NADH was monitored at 340 nm. In the case where thio-NAD was used as a substrate for the reaction, production of thio-NADH was monitored at 395 nm (E_{395} = 11.3 mM^{-1} cm^{-1}).

Velocity as a function of enzyme concentration was determined in the direction of oxidative decarboxylation at pH 4.4, 7.5, and 9.8. In all cases, the activity per milliliter determined equally reflected the rate of NAD–malic enzyme. Oxidative decarboxylation was assayed by using 100 mM Hepes, pH 7.3, 1.0 mM DTT, 154 mM malate (28 mM when corrected for Mg–malate), 13.4 mM NAD (2 mM when corrected for Mg–NAD), and 250 mM $MgSO_4$ (112 mM when corrected for Mg–malate and Mg–NAD). Further, competing lactate dehydrogenase (LDH) and malate dehydrogenase (MDH) activities were found to be insignificant (less than 5% of the total activity).

pH Studies. Determination of V and V/K for NAD (or thio-NAD) and malate were carried out by varying the levels of the desired substrate at saturating concentrations of all others. The K_i values for inhibitors vs. malate were determined with NAD and Mg^{2+} saturating, varying the concentrations of malate at several different inhibitor concentrations including zero. Individual experiments will be discussed in further detail under Results. All assays reflected initial velocity conditions with less than 10% of the limiting reactant utilized over the time course of the reaction. The pH ranges of the buffers (100

[2] Substrate stickiness is observed when substrate dissociates slower than it reacts to give products.

mM) used to obtain the pH profiles were as follows: *N,N'*-bis(2-hydroxyethyl)piperazine, 4.0–5.5; Mes, 5.5–6.5; Pipes, 6.5–7.5; Hepes, 7.0–8.0; Taps, 8.0–9.0; Ches, 9.0–10.0; BTP, 9.0–10.0; Caps, 10.0–11.0. All buffers were titrated to pH with KOH. In all cases, sufficient overlaps were obtained when buffers were changed so that correction could be made for spurious buffer effects. The pH of the reaction mixture was measured with a Radiometer PHM82 pH meter with a combined microelectrode before and after sufficient data were collected for determination of initial velocities. Negligible pH changes were observed before and after reaction.

Since total substrate and inhibitor concentrations were somewhat high in some cases (particularly at low pH), substrate and inhibitor stock solutions were titrated to the approximate pH value of the assay. Above pH 8.5, NAD was preequilibrated at 25 °C and added to the reaction mixture just prior to the addition of enzyme to minimize the base-catalyzed degradation of the nucleotide. No significant effect of ionic strength was observed up to 3.5 M.

It was important to determine the stability of the enzyme over the pH range studied since this could potentially give rise to incorrectly determined values of the kinetic parameters as well as the inhibition constants for inhibitors. Thus, NAD–malic enzyme was incubated with the buffer systems to be utilized for up to 25 min. During that time aliquots were removed and assayed for activity in the direction of oxidative decarboxylation at pH 7.3, a pH where the enzyme was known to be stable (Landsperger et al., 1978). The only significant decrease in activity occurred at the pH extremes (pH 4.3 and below or pH 10.4 and above) yielding a $T_{1/2}$ for inactivation of 14 min at pH 4.3 and 17.6 min at pH 10.4. However, even at pH values where the enzyme is less stable, initial velocity data can be obtained since the pH-jump technique was utilized for all assays in this study. According to this technique, enzyme is kept in dilute buffer solution at pH 7.3 and the reaction is initiated by addition of enzyme to the reaction mixture containing 100 mM buffer at the pH being studied.

An estimate of the variation of the kinetic mechanism over the pH range to be studied is required in order to ensure one knows which enzyme complex is being titrated. Thus, an initial velocity pattern was obtained (data not shown) at pH 5.3 by varying all three reactants[3] systematically and analyzing the data according to the method of Viola & Cleland (1982). The K_B, coeff C, and K_{1C} terms (Park et al., 1984) are undefined in the denominator of the rate equation (see eq 3, below). This is in agreement with the data of Park et al. (1984). Thus, the kinetic mechanism as described by Park et al. (1984) is pH-independent over the pH range 5.3–9.0.

Data Analysis. Reciprocal initial velocities were plotted as a function of reciprocal substrate concentrations. Data were analyzed by using the appropriate rate equations and whenever possible by using the Fortran programs of Cleland (1979). The points in the figures are the experimentally determined values, while the curves are calculated from fits of the data by using the appropriate equation. Data conforming to a straight line were fitted by using the equation for a straight line. Individual saturation curves used to obtain the pH profiles were fitted by using eq 1. Data conforming to rapid equilibrium ordered

$$v = \frac{VA}{K + A} \tag{1}$$

addition of the metal prior to malate were fitted by using eq 2. Terreactant initial velocity data were first analyzed

$$v = \frac{VAB}{K_{ia}K_b + K_bA + AB} \tag{2}$$

graphically according to Viola & Cleland (1982) and then fitted by using eq 3, which describes a fully random terreactant mechanism. Data for linear competitive and noncompetitive

$$v = VABC/[\text{const} + (\text{coeff } A)A + (\text{coeff } B)B + (\text{coeff } C)C + K_aBC + K_bAC + K_cAB + ABC] \tag{3}$$

inhibition were fitted by using eq 4 and 5, respectively. In

$$v = \frac{VA}{K(1 + I/K_{is}) + A} \tag{4}$$

$$v = \frac{VA}{K(1 + I/K_{is}) + A(1 + I/K_{ii})} \tag{5}$$

eq 1–5, A, B, and C are reactant concentrations, and I is inhibitor concentration; K_a, K_b, and K_c are Michaelis constants and K_{ia}, K_{is}, and K_{ii} are inhibition constants for A, slope, and intercept, respectively. In eq 3, the constant and coefficient terms are lumped kinetic constants that are dependent on mechanism. Data for pH profiles that decreased with a slope of 1 at low pH and a slope of −1 at high pH were fitted by using eq 6. Data for pH profiles that decreased with a slope of 1 at low pH were fitted by using eq 7, while data for pH profiles that decreased with a slope of −1 at high pH were fitted by using eq 8. Data for pK_i profiles in which pK_i decreased from a constant value at one pH to another constant value at another pH were fitted by using eq 9. In eq 6–8, K_1 and K_2

$$\log y = \log \frac{C}{1 + [\text{H}]/K_1 + K_2/[\text{H}]} \tag{6}$$

$$\log y = \log \frac{C}{1 + [\text{H}]/K_1} \tag{7}$$

$$\log y = \log \frac{C}{1 + K_1/[\text{H}]} \tag{8}$$

$$\log y = \log \frac{Y_L + Y_H(K_1/[\text{H}])}{1 + K_1/[\text{H}]} \tag{9}$$

represent the dissociation constants for enzyme groups, y is the value of the parameter observed as a function of pH, and C is the pH-independent value of y. In eq 9, K_1 is the dissociation constant for an enzyme or substrate group, and Y_L and Y_H are the observed values of y at low and high pH, respectively. Initial velocities obtained by varying the concentration of deuterium-labeled or unlabeled L-malate at saturating levels of Mg^{2+} and NAD, or those obtained at saturating levels of Mg^{2+} and deuterium-labeled or unlabeled L-malate by varying the concentration of NAD, were fitted by using eq 10 and 11. These equations assume independent

$$v = \frac{VA}{K(1 + F_iE_{V/K}) + A(1 + F_iE_V)} \tag{10}$$

$$v = \frac{VA}{(K + A)(1 + F_iE_{V/K})} \tag{11}$$

isotope effects on V and V/K (eq 10) or equal effects on both V and V/K (eq 11). In eq 10 and 11, F_i is the fraction of deuterium label in substrate, while E_V and $E_{V/K}$ are the isotope effect minus 1 for the respective parameters. In all cases, the best fit of the data was chosen on the basis of the lowest values of the standard errors of the fitted parameters and the lowest

[3] Although Mg^{2+} is not transformed during the course of the reaction, the rate is directly dependent on the uncomplexed divalent metal concentration. Therefore, Mg^{2+} can be considered a pseudoreactant.

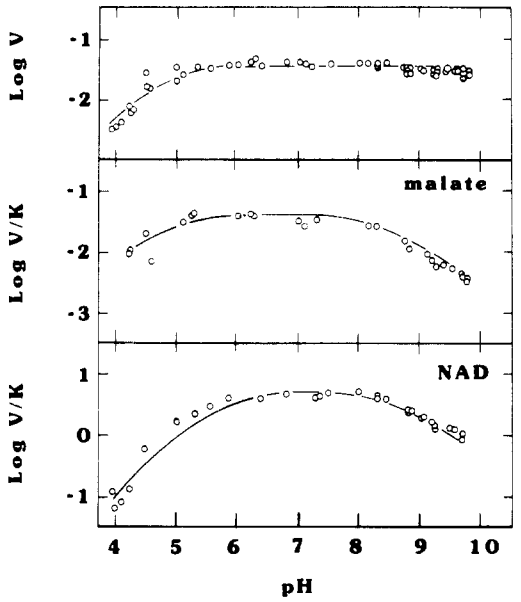

FIGURE 1: pH dependence of the kinetic parameters with NAD as the nucleotide substrate. The V/K value for malate was obtained at saturating concentrations of NAD (2.0 mM) and Mg^{2+} (180 mM, pH 5.3 and below; 360 mM, pH 6.0–8.3; 40 mM, pH 8.8 and above) while the concentration of malate was varied around its K_m (2–20 mM, pH 5.2 and below; 0.5–5.0 mM, pH 6.0–8.3; 5–50 mM, pH 8.8 and above). The V/K value for NAD was obtained at saturating concentrations of malate (37 mM, pH 4.5 and below; 25 mM, pH 5.0–8.3; 90 mM, pH 8.8 and above) and Mg^{2+} (180 mM, pH 8.3 and below; 80 mM, pH 8.8 and above) while the concentration of NAD was varied around its K_m (0.01–0.1 mM). All substrate concentrations were corrected for the amount of metal chelate complex as described under Materials and Methods. The points shown are the experimentally determined values, while the curves are from a fit of the data using eq 6 for V/K values and eq 7 for V values.

value of σ. σ is defined as the sum of the squares of the residuals divided by the degrees of freedom, where degrees of freedom is equal to the number of points minus the number of parameters (Cleland, 1979).

RESULTS

pH Dependence of Kinetic Parameters. The pH dependence of the kinetic parameters for the ascarid NAD–malic enzyme was determined, and the results are shown in Figure 1. The maximum velocity is pH-dependent and decreases below a pK of 4.8 ± 0.03. The V/K for malate decreases below a pK of 4.7 ± 0.3 and above a pK of 8.7 ± 0.2. The pK for the 4-carboxyl group of malate is also reflected in V/K_{malate}; that is, the V/K decreases with a slope of 2 at low pH. This latter pH dependence has been subtracted out of the data displayed in Figure 1 by using a pK of 4.7 for malate (Martell & Smith, 1977). The V/K for NAD decreases below a pK of 5.7 ± 0.1 and above a pK of 8.9 ± 0.1. The pH-independent values of these parameters are $V/E_t = 38\ s^{-1}$, $V/(K_{malate}E_t) = 3.8 \times 10^4\ M^{-1}\ s^{-1}$, and $V/(K_{NAD}E_t) = 3.8 \times 10^6\ M^{-1}\ s^{-1}$.

In addition to the parameters discussed above, the pH dependence of Mg^{2+} binding was also determined, and the results are shown in Figure 2. The K_i for Mg^{2+} increases upon protonation of an enzyme group (or groups) with a pK of 9.8 ± 0.1. The K_i is 0.82 ± 0.016 mM when this group is not protonated and 16.1 ± 0.2 mM when the group is protonated. When Mg^{2+} is bound to enzyme, the pK is perturbed to 8.5 ± 0.1. Additionally, there is a further increase in the K_i for Mg^{2+} below pH 5.3. A value of 140 mM was obtained at pH 4.3.

The divalent metals Mn^{2+} and Cd^{2+} can also be utilized by NAD–malic enzyme. V with Mn^{2+} increases about 2-fold over

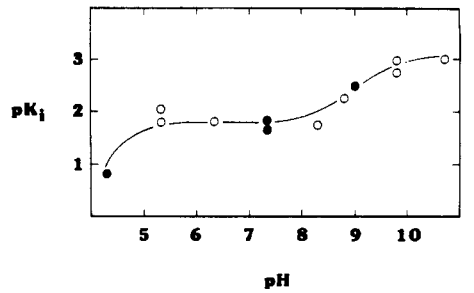

FIGURE 2: pH dependence of the Mg^{2+} dissociation constant. The closed circles represent data fitted by using eq 1, which were obtained at saturating concentrations of NAD (2.0 mM) with malate equal to one-tenth its K_m (0.1 mM) while the concentration of Mg^{2+} was varied from 10 to 100 mM at pH 7.5 and from 1 to 10 mM at pH 9.0 (under these conditions $K_{Mg} = K_{i\,Mg}$). Open circles represent data fitted by using eq 2, obtained at saturating concentrations of NAD (2.0 mM) while the concentration of Mg^{2+} was varied (10–100 mM, pH 5.3; 5–50 mM, pH 6.3 and 8.3; 1–10 mM, pH 8.8 and above), as was that of malate (0.5–5.0 mM, pH 5.3; 1–10 mM, pH 6.3 and 8.3; 10–100 mM, pH 8.8 and above). All substrate concentrations were corrected for the amount of metal chelate complex as described under Materials and Methods. The curve is a theoretical fit of the Mg^{2+} K_i values to eq 9 from pH 6 to 10 and eq 7 for data from pH 7 and below.

that with Mg^{2+}, and it decreases 40% with respect to Mg^{2+} in the case of Cd^{2+}. The pH dependence of the kinetic parameters from pH 4.5 to 6.0 (data not shown) indicates that K_{malate} does not change when either metal is used. When Mn^{2+} is the divalent metal, K_{malate} is ca. 0.2 mM, and K_{malate} is 1 mM when Cd^{2+} is used. K_i for the metal is also pH-independent with a value of 0.15 mM for Cd^{2+} and 1.5 mM for Mn^{2+}.

The ascarid NAD–malic enzyme will use thio-NAD as a slow alternate reactant (Park et al., 1984), being used at a maximum velocity which is 5% that of NAD. As shown in Figure 3, V for thio-NAD is pH-independent from pH 4.2 to 9.6 while $V/K_{thio\text{-}NAD}$ decreases below a pK of 5.6 ± 0.1 and above a pK of 9.0 ± 0.2. The pH-independent value of V/E_t when thio-NAD is the reactant is 1.9 s^{-1}, while the pH-independent value of $V/(K_{thio\text{-}NAD}E_t)$ is $5.4 \times 10^5\ M^{-1}\ s^{-1}$.

pH Dependence of Inhibition. The pH dependence of the dissociation constants for tartronate and oxalate (inhibitors vs. malate) were determined. From the inhibition patterns obtained at pH 4.4, 4.9, 8.0, and 9.3 it was shown that tartronate inhibition vs. malate is competitive. The pK_i profile for tartronate inhibiton is shown in Figure 4A. K_{is} for tartronate increases below a pK of 4.8 ± 0.2 and above a pK of 9.0 ± 0.2, while the pH-independent value of K_{is} is 1.1 ± 0.06 mM.

The type of inhibition one observes for oxalate vs. malate is pH- and nucleotide-dependent. A competitive inhibition pattern is obtained at pH 8.5, with a K_{is} value of 126 ± 8 μM. However, as the pH decreases below pH 7, noncompetitive inhibition is obtained. The K_{is} and K_{ii} values obtained from these data at pH 6.4 are 52 ± 5 and 285 ± 50 μM, respectively. From experiments similar to those described above, the pH dependence of the K_i values for oxalate inhibition was obtained, and the results are shown in Figure 4B. K_{ii} is pH-dependent, increasing above an apparent pK of 4.9 ± 0.2. K_{is} for oxalate is calculated to be 3 μM by assuming a pK of 4.9 for protonation of the enzyme–metal–nucleotide complex. When this complex is deprotonated, the K_{is} value increases to 0.16 mM. The pK for protonation of the enzyme–metal–nucleotide complex is perturbed to 6.7 when oxalate is bound.

At pH 6.3, with thio-NAD as the nucleotide the inhibition by oxalate vs. malate is competitive (data not shown). This is in contrast to the noncompetitive inhibition observed when

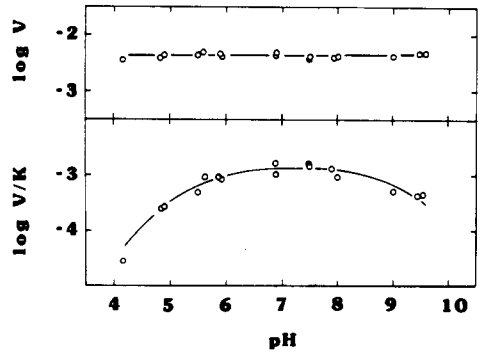

FIGURE 3: pH dependence of V and V/K for thio-NAD. The concentration of thio-NAD was varied around its K_m (0.005–0.05 mM) at saturating concentrations of Mg^{2+} (180 mM) and malate (20 mM below pH 8.5 and 125 mM above). All substrate concentrations were corrected for the amount of metal chelate complex formation as described under Materials and Methods. Each assay was initiated by addition of NAD–malic enzyme (84 nM final concentration). The points shown are the experimentally determined values while the curve for V/K is from a fit of the data using eq 6. For V, the line represents the average value of the parameter.

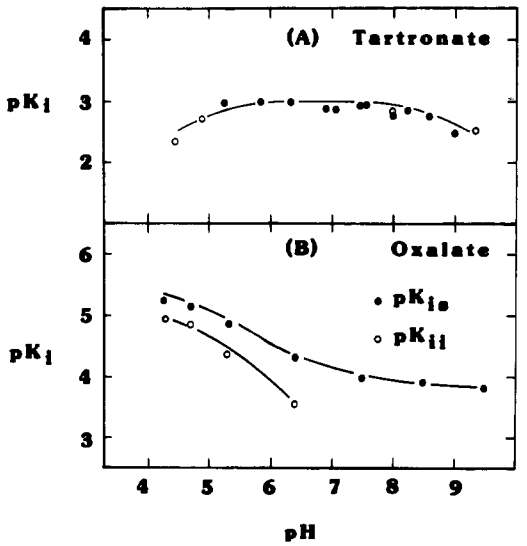

FIGURE 4: pH dependence of inhibitor dissociation constants for NAD–malic enzyme. (A) pH dependence of the tartronate dissociation constant. The open circles represent data obtained from full inhibition patterns. Malate was varied (1–10 mM, pH 8.0 and 9.5; 2–20 mM, pH 4.4) with NAD (1.0 mM) and Mg^{2+} (180 mM, pH 4.4 and 8.0; 18 mM, pH 9.5) at saturating concentrations. Tartronate was fixed at 0.5, 1.0, and 2.0 mM (pH 9.5), 1.0, 2.0, and 4.0 mM (pH 8.0), or 2.0, 4.0, and 8.0 mM (pH 4.4). The closed circles represent data from Dixon plots varying tartronate (1.0–4.0 mM) at saturating levels of NAD (2.0 mM) and Mg^{2+} (180 mM) with malate at its K_m (1.0 mM). Under these conditions, the true K_i is half the experimentally obtained value. The data points are the experimentally determined values while the curve is from a fit of the data using eq 6. (B) pH dependence of the oxalate dissociation constants. All data are from full inhibition patterns. Data in the pH range 4.3–8.5 were obtained with malate varied (1–10 mM) at fixed levels of oxalate 0.1, 0.2, 0.4 mM) and Mg^{2+} (180 mM) and NAD (1.0 mM) saturating. At pH 9.5, Mg^{2+} and NAD were fixed at 50 and 1.0 mM, respectively. Above pH 7.0, the data were fitted by using eq 4, while below pH 7.0 the data were fitted by using eq 5. The resulting $1/K_{ii}$ values (○) were fitted by using eq 8 (theoretical curve through the data). The curve for $1/K_{is}$ (●) was drawn from an eye fit of the data after analysis (see Discussion). All substrate and inhibitor concentrations were corrected for metal chelate complex formation as described under Materials and Methods.

NAD is utilized as the nucleotide. The consequence of this change in the type of inhibition one observes depending on the nucleotide will be further discussed in terms of the kinetic mechanism under Discussion.

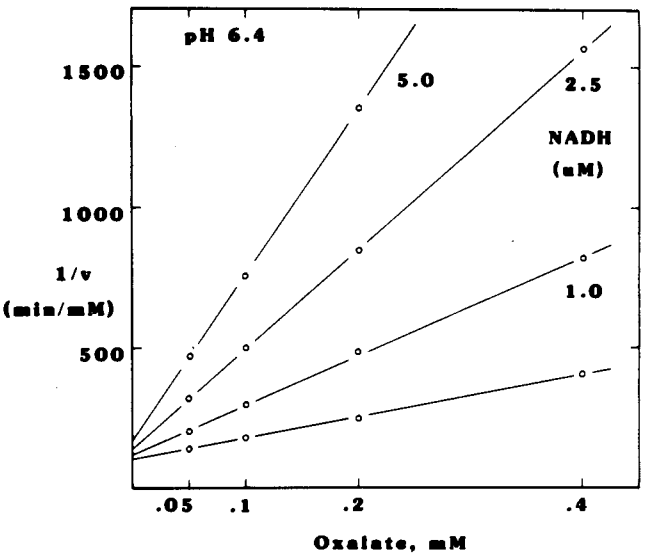

FIGURE 5: Double inhibition by oxalate and NADH at pH 6.4. Substrate concentrations were as follows: NAD, 0.1 mM; Mg^{2+}, 180 mM; malate, 1.25 mM. All substrate and inhibitor concentrations were corrected for the amount of metal chelate complex formation as described under Materials and Methods. The points shown are the experimentally determined values while the curves are from a fit of the data using eq 5.

Table I: Primary Deuterium Isotope Effects for *Ascaris suum* NAD–Malic Enzyme

substrate	^{D}V	$^{D}(V/K)^{a}$	$^{D}V = {}^{D}(V/K)^{b}$
malate	1.45 ± 0.02[c]	1.58 ± 0.26	1.45 ± 0.04
NAD	1.45 ± 0.02[c]	1.52 ± 0.25	1.49 ± 0.03
thio-NAD	1.70 ± 0.1[a]	1.67 ± 0.26	1.69 ± 0.04

[a] Values listed are the average pH-independent value from a fit of the data to eq 12. [b] Values listed are the average pH-independent value from a fit of the data to eq 13. [c] Average pH-independent value from a fit of the $^{D}V - 1$ data to eq 7.

Double Inhibition. These types of experiments were first described by Yonetani & Theorell (1964) and can be utilized to obtain information on the form of the enzyme to which inhibitors are binding. For these experiments, if the inhibitors bind to different forms of the enzyme, a series of parallel lines will be obtained when $1/v$ is plotted as a function of the first inhibitor concentration at different fixed levels of the second inhibitor. If both inhibitors can simultaneously bind to the same form of the enzyme, an intersecting pattern will be obtained. As can be seen in Figure 5, there is a pronounced enhancement of oxalate inhibition in the presence of NADH at pH 6.4 as evidenced by the increase in the slope with increasing NADH concentration. Thus, both NADH and oxalate can bind to form an E–NADH–Mg–Ox complex.

pH Variation of Deuterium Isotope Effects. The primary deuterium isotope effects were measured as a function of pH. The V isotope effect decreases to a limiting value of 1 at low pH. Therefore, 1 was subtracted from all ^{D}V values, and the resulting values of $^{D}V - 1$ were fitted by using eq 7 in order to obtain the pK value for this process. The value of log ($^{D}V - 1$) decreases below a pK of 4.9 ± 0.07, while both $^{D}(V/K_{malate})$ and $^{D}(V/K_{NAD})$ are pH-independent and equal to the pH-independent value of ^{D}V. As a result, data above pH 7 were fitted by using eq 11. The pH variation of the primary deuterium isotope effects using the slow alternate nucleotide thio-NAD was also obtained. These effects are pH-independent over the pH range measured (4.7–7.4). The average pH-independent values of the parameters are listed in Table I.

Discussion

pH Dependence of Kinetic Parameters. For a mechanism in which substrate binds to only the correctly protonated form of the enzyme, the V profile will be pH-independent and the pK values for catalytic and binding groups will only be displayed in the V/K profile (Cleland, 1977; Cook & Cleland, 1981b). Under these conditions the pK values obtained from the V/K profile are intrinsic (Cleland, 1977). The V profile for the slow substrate thio-NAD is pH-independent as shown in Figure 3. Thus, it appears that substrates bind to only the correctly protonated form of the enzyme and the pK values of 5.6 and 9.0 observed in the $V/K_{\text{thio-NAD}}$ profile are true pK values for enzyme groups. Further, since the V/K for thio-NAD is obtained at saturating Mg^{2+} and malate, these pK values reflect enzyme residues in the E–Mg–malate complex.

In contrast, when NAD is the reactant, the V profile (Figure 1) is pH-dependent, displaying a pK value of 4.8. There are two possibilities for the pH dependence observed in the V_{NAD} profile. Since the pK value observed in the V profile is essentially the same as that seen for V/K_{malate} (4.7), it is possible that different protonation states of malate bind equally well to enzyme but only the correctly protonated form of the substrate is catalytically competent and, in essence, one observes a substrate pK in the V profile. However, since this pK is not observed for thio-NAD, and since malate is the other substrate in both cases, this is extremely unlikely. Alternatively, some step after catalysis is pH-dependent and becomes rate-determining with NAD as the substate, as a group with an apparent pK of 4.8 becomes protonated. Possibilities for this slow step include a pH-dependent release of a product after release of the first product or a pH-dependent isomerization of free enzyme or an enzyme–substrate complex. The first product released will likely be CO_2 so that the slow step could involve release of either pyruvate or NADH. It has been shown for a number of NAD(P)-dependent dehydrogenases that release of NAD(P)H is at least partially rate-determining. For example, Schimerlik & Cleland (1977a) have shown for pigeon liver malic enzyme that NADPH release is 25 times slower than catalysis and limits the overall reaction. The deuterium isotope effect on V in this case is 1.0. This cannot be true for the ascarid enzyme since a finite isotope effect of 1.45 is observed on V.

The pK values observed in the V/K profile for NAD are 5.7 and 8.9, essentially the same as those observed for $V/K_{\text{thio-NAD}}$. This is consistent with a mechanism that requires binding to only the correctly protonated form of the enzyme as stated above.

In addition, thio-NAD is a slow substrate, a decrease in the catalytic rate of 20-fold (going from NAD to thio-NAD) does not change the pK values, and thus, even with NAD as the substrate, true pK values are observed. The pK values observed in the V/K profile for NAD (just as for thio-NAD) represent enzyme groups in E–Mg–malate, while pK values observed in the V/K profile for malate represent enzyme groups in the E–Mg–NAD complex. Although the basic pK (8.7–9.0) is not sensitive to what is bound to enzyme, the acidic pK is 4.7 when NAD is bound and 5.6 when malate is bound. This same group has a pK of 5.6 in free enzyme (Park, 1985). Thus, the pK for this group is perturbed to a lower pH when nucleotide is bound.

Interpretation of Inhibition Data. In order to further test the hypothesis that the pK values obtained from the pH dependence of the kinetic parameters, particularly V/K_{malate}, are intrinsic, the pH dependence of the K_i for tartronate, a structural analogue and competitive inhibitor of malate, was obtained (Figure 4A). Since this inhibition is competitive, it is only observed under conditions where substrate is limiting and, thus, where all steps prior to addition of substrate come to thermodynamic equilibrium. As a result, true pK values are observed for the pH dependence of K_i values for competitive inhibitors (Cleland, 1977) and can be used to check whether or not the observed pK values in the substrate profile are true pK values if the protonation state of these groups affects inhibitor binding. The pK values obtained from the pK_i tartronate profile are essentially the same as values observed for the V/K_{malate} profile. Thus, the observed pK values in the V/K_{malate} profile are indeed intrinsic.

The pH dependence of oxalate inhibition vs. malate was also determined. Oxalate is a structural analogue of the enolate of pyruvate, a putative intermediate for the malic enzyme reaction (Hsu, 1982). As shown in Figure 4B, this inhibition is quite complex, and one obtains both competitive inhibition above pH 7 and noncompetitive inhibition below pH 7. The intercept inhibition observed below pH 7 indicates combination to an enzyme form present when all substrates are saturating. Since oxalate competes with malate at all pH values (slope inhibition) for the E–NAD–Mg complex, the most likely candidate for the product complex to which oxalate binds is the E–NADH–Mg complex, which is structurally very similar to the oxidized nucleotide complex. As a result, if NADH release becomes slower as the pH decreases, more E–NADH–Mg will be present to which oxalate can bind, and the intercept effect should become more pronounced. Thus, the product complex being titrated in the V profile displaying a pK of 4.8 is most likely E–NADH–Mg, and this will be further shown below.

The pH-independent value of K_{is} for oxalate at high pH is ca. 0.16 mM, making oxalate the tightest binding inhibitor found to data. The inhibition vs. pH profile is quite different from that observed for tartronate. For optimal binding, oxalate requires the group with a pK of 4.8 observed in the V/K_{malate} and pK_i tartronate profiles to be protonated as opposed to malate and tartronate, which require this group to be unprotonated. Since true pK values are observed for this kind of pH profile, the pK for this group must be 4.8 as it is for the V/K_{malate} and pK_i tartronate profiles. The pH dependence of oxalate inhibition (pK_{is} profile) adheres to the following:

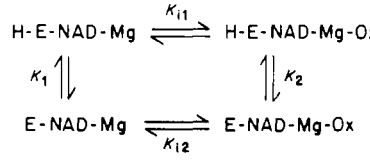

(12)

where K_1 and K_2 are the acid dissociation constants of the enzyme group in the H–E–NAD–Mg and H–E–NAD–Mg–Ox complexes, respectively, while K_{i1} and K_{i2} are the dissociation constants for oxalate from the protonated and unprotonated species, respectively. The combination of both the proton and oxalate to enzyme is at equilibrium in the steady state, and thus, $K_{i2}K_2 = K_{i1}K_1$. A value of 0.16 mM is obtained from the pK_{is} profile as the pH-independent value of K_{i2} (the value where the profile levels off at high pH). The pH at which K_i decreases to 0.08 mM represents K_2 (pK_2 = 6.7). The value of pK_1 must be 4.8 as is observed for this group in the V/K_{malate} and pK_i tartronate profiles. As a result, a value of 2 μM is calculated for K_{i1}. Since oxalate binds tighter when the group in the E–NADH–Mg and E–NAD–Mg complexes becomes protonated, the group being protonated is most likely the same in both cases. It is interesting to note that the pK_{is} profile for oxalate does not reflect the pH dependence of the

group with a pK of 9 as is observed in both the V/K_{malate} and pK_i tartronate profiles. The consequences of this will be discussed in detail in terms of the chemical mechanism (below).

Since oxalate appears to be binding to E–NADH–Mg below pH 7, addition of NADH to the reaction mixture should enhance the inhibition observed. The data in Figure 5 show conclusively that E–NADH–Mg–Ox can form. This is in agreement with the hypothesis that as the pH is decreased the release of NADH becomes more rate-determining and thus, at pH 4, NADH release limits the overall reaction rate. Conversely, with thio-NAD the catalytic pathway is rate-limiting, and thus no significant amount of E–thio-NAD-Mg is accumulated in the steady state. Therefore, oxalate inhibition vs. malate is predicted to be competitive over the entire pH range. As stated under Results, at pH 6.4 competitive inhibition is observed when thio-NAD is utilized as the nucleotide. Again, this is in agreement with the aforementioned hypothesis.

Deuterium Isotope Effects. Cook & Cleland (1981a,b,c) have developed the theoretical basis for establishing the protonation mechanism for an enzyme-catalyzed reaction from the pH variation of the primary isotope effects. However, one must first have data on the pH dependence of the kinetic parameters and K_i values for inhibitors in order to establish a frame of reference for proper interpretation of the isotope effects. Isotope effect data can also yield information that will be helpful toward elucidation of the rate-determining steps along the enzymatic reaction coordinate. The pK values obtained from the pH variation of the kinetic parameters are the reference points in evaluating the isotope effect data. As listed in Table I, ^DV and $^D(V/K)$ for thio-NAD are equal and pH-independent over the range measured. These data are consistent with a mechanism for NAD–malic enzyme in which substrates bind to only the correctly protonated form of the enzyme.

The value for ^DV decreases to 1 at pH 4 as expected if product release, which is not isotope-sensitive, becomes rate-limiting. The differences between ^DV and $^D(V/K)$ is the c_{vf} vs. c_f term.[4] The expression for c_{vf} is

$$c_{vf} = k_{cat}/k_{off\ pyruvate} + k_{cat}/k_{off\ NADH} \qquad (13)$$

It is c_{vf} that is becoming larger at low pH, but as suggested above, most likely only the off-rate for NADH is slow enough to be observed. As shown above for oxalate inhibition, it would be expected that $k_{cat}/k_{off\ NADH}$ would become larger at low pH since protonation of the group with a pK of 4.8 slows down release of NADH. Thus, NADH release is partially rate-determining at pH values above 7 and becomes more rate-determining with decreasing pH, until at pH 4 it limits the overall reaction rate.

As shown by Cook & Cleland (1981a), kinetic isotope effects are also a powerful tool in determining kinetic mechanism. Consider a steady-state ordered mechanism with A adding to enzyme prior to addition of B. For this mechanism, V/K_a is the pseudo-first-order rate constant for addition of A to free enzyme (k_{on}) and, therefore, contains no catalytic component. Thus, there will be no isotope effect on V/K_a [$^D(V/K_a) = 1$]. Moreover, for any bi- or terreactant enzyme, if one measures a finite isotope effect on all V/K values, one can conclude that the mechanism is random (Cook & Cleland, 1981a). For NAD–malic enzyme, the $^D(V/K)$ values for NAD and malate are finite and equal to the pH-independent value of ^DV. Thus, the kinetic mechanism for NAD–malic enzyme in the direction of oxidative decarboxylation is random. Furthermore, since the isotope effects are all equal, the off-rates for NAD and malate from the quaternary complex must be equal to the off-rate for NADH from E–NADH, or the off-rates must all be much greater than the catalytic steps; that is, the mechanism is rapid-equilibrium random. However, data of Park et al. (1984) indicate a steady-state random mechanism. In addition, data recently obtained by using the isotope partitioning method of Rose et al. (1974) indicate that NAD is somewhat sticky from the quaternary E–NAD–Mg–malate complex, being released 2-fold slower than the catalytic rate.[5] Thus, c_{vf} is finite, and since all isotope effects are equal, the off-rates for NAD, malate, and NADH from their respective complexes must be equal.

The primary deuterium isotope effects for the ascarid enzyme with NAD as the nucleotide are 1.45 and equal. When thio-NAD is utilized, the maximum velocity is decreased 20-fold while the isotope effects are only increased to 1.7. There are a number of possibilities as to why this occurs. Obviously, hydride transfer is not solely rate-limiting with either nucleotide, and whatever step is contributing to the rate limitation must be included in both V and V/K since ^DV is equal to $^D(V/K)$ with both nucleotides.

Scheme I

$$EABC \underset{k_{8a}}{\overset{k_{7a}}{\rightleftharpoons}} E'ABC \underset{k_{8b}}{\overset{k_{7b}}{\rightleftharpoons}} E'BXQR \xrightarrow{k_{7c}} E'BQR$$

The catalytic pathway can be depicted as shown in Scheme I, where A, B, C, Q, R, and X are NAD, Mg^{2+}, malate, pyruvate, NADH, and oxalacetate, respectively. Here k_{7a} represents a substrate-induced conformational change in the Michaelis complex, while k_{7b} is hydride transfer and k_{7c} is decarboxylation of oxalacetate and release of CO_2. It is possible that both decarboxylation and hydride transfer are slowed down by the same amount upon replacement of NAD with thio-NAD. However, it is difficult to imagine a substitution on the nicotinamide ring of NAD affecting decarboxylation and/or release of CO_2. Alternatively, there may be a change in the transition state for hydride transfer from late to early (consistent with the decrease in redox potential in going from NAD to thio-NAD) that could account for the small change in the observed isotope effect as a result of nucleotide substitution. Hermes et al. (1984) and Scharschmidt et al. (1984) have shown that for selected dehydrogenases even though there is an increase in the intrinsic deuterium isotope effect as the redox potential of the nucleotide becomes more positive, the observed values of ^DV and $^D(V/K)$ may not change significantly.

The most likely possibility that may explain the lack of a large change in the observed deuterium isotope effect is that k_{7a} in the catalytic pathway may be decreased upon substi-

Scheme II

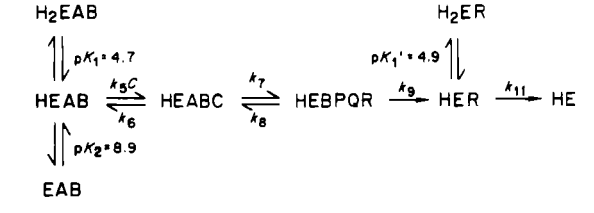

[4] The c_{vf} term is a summation of the ratios of the catalytic rate constant to any unimolecular step in the forward direction at saturating substrate concentrations. The c_f term is the ratio of the catalytic rate to the net rate constant for substrate release from the Michaelis complex.

[5] Unpublished results of C. Y. Chen in this laboratory.

tution with thio-NAD. That is, the enzyme may no longer be able to undergo, as effectively, the conformational change necessary for catalysis. Finally, there may be a large degree of nonproductive binding with thio-NAD as the nucleotide substrate.

Protonation Mechanism. The above data support the proposed protonation mechanism shown in Scheme II for *Ascaris suum* NAD–malic enzyme, where A, B, C, P, Q, and R are NAD, Mg^{2+}, malate, CO_2, pyruvate, and NADH, respectively. All catalytic interconversions are represented by k_7 and k_8. Included in k_9 are all product-release steps except NADH release, which is represented by k_{11}. According to the net rate constant method of Cleland (1975) the rate equation for the above mechanism is

$$v = k_7C/[K_i(1 + k_7/k_6 + k_8/k_9)(1 + [H]/K_1 + K_2/[H]) + [1 + k_7/k_9 + k_7/k_{11}(1 + [H]/K_1') + k_8/k_9]C] \quad (14)$$

where K_i represents the dissociation constant for malate from E–NAD–Mg–malate. For this mechanism, V and V/K for malate are

$$V = k_7/[1 + k_7/k_9 + k_7/k_{11}(1 + [H]/K_1') + k_8/k_9] \quad (15)$$

$$V/K = k_7/[K_i(1 + k_7/k_6 + k_8/k_9)(1 + [H]/K_1 + K_2/[H])] \quad (16)$$

A similar expression can be derived for V/K_{NAD}.

The off-rates for both CO_2 and pyruvate are represented by k_9 in Schem II. Estimates of the K_m values for both of these substrates of the reverse reaction have been obtained (Park, 1985), and it is known they are quite large (ca. 10 mM). It is also predicted that the kinetic mechanism for NAD–malic enzyme in the reverse direction is rapid-equilibrium random (Park et al., 1984). Thus, for both of these substrates, $K_m = K_i$. Moreover, if we assume a diffusion-limited on-rate for these substrates, the off-rates must be very fast (ca. 1×10^5 s^{-1}). Therefore, we predict k_9 to be much greater than either k_7 or k_8 and can write simplified expressions for both V and V/K:

$$V = \frac{k_7}{1 + k_7/k_{11}(1 + [H]/K_1')} \quad (17)$$

$$V/K = \frac{k_7}{K_i(1 + k_7/k_6)(1 + [H]/K_1 + K_2/[H])} \quad (18)$$

From these expressions, we predict both V and V/K to be pH-dependent, with V and $^DV - 1$ decreasing below pK_1'. In addition, while V/K decreases below pK_1 and above pK_2, the isotope effect on V/K is pH-independent. Further, since the primary deuterium isotope effects on V/K and V are equal, we can conclude that $k_6 = k_{11}$. The overall reaction rate above pH 7 must be partially limited by k_{11} since a small pH change below pH 7 results in the observation of noncompetitive inhibition by oxalate. The observed pK_1' is an apparent pK described as

$$pK_1'(app) = pK_1' - \log(1 + k_{11}/k_7) \quad (19)$$

A true pK is not observed in the V profile, but it can be calculated since an estimate of the value for k_{11}/k_7 is known. As stated above, recent isotope-partitioning experiments indicate c_f for NAD ($k_7/k_{off\,NAD}$) is ca. 2, and since c_f is equal to c_{of}, k_7/k_{11} must also be 2. Thus, pK_1' is calculated as about 5. This value is, within experimental error, essentially equal to the observed value of 4.8, indicating that small amounts of substrate or product stickiness can be missed by using a comparison of pK values. The limits of the pH-dependent rate equation for NAD–malic enzyme from *Ascaris suum* are shown in Table II.

Table II: Limits of the Rate Equation for NAD–Malic Enzyme

parameter	pH low	pH neutral	pH high
V	$k_{11}K_1/[H]$	$k_7/(1 + k_7/k_{11})$	$k_7/(1 + k_7/k_{11})$
^DV	1.0	$(^Dk_7 + k_7/k_{11})/(1 + k_7/k_{11})$	$(^Dk_7 + k_7/k_{11})/(1 + k_7/k_{11})$
V/K_{malate}	$k_7K_1/K_i(1 + k_7/k_6)[H]$	$k_7/K_i(1 + k_7/k_6)$	$k_7[H]/K_i(1 + k_7/k_6)K_2$
$^D(V/K_{malate})$	$(^Dk_7 + k_7/k_6)/(1 + k_7/k_6)$	$(^Dk_7 + k_7/k_6)/(1 + k_7/k_6)$	$(^Dk_7 + k_7/k_6)/(1 + k_7/k_6)$

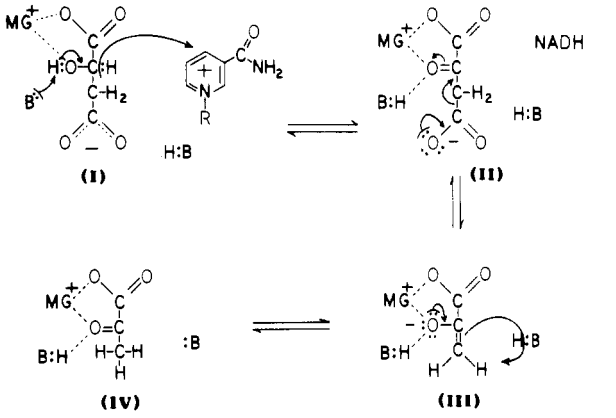

FIGURE 6: Proposed chemical mechanism for NAD–malic enzyme. The scheme is not meant to imply correct geometry or stereochemistry but simply to show the movement of protons and electrons.

For NAD–malic enzyme from *Ascaris suum*, the protonation state of the groups observed in the V/K profiles can be unambigiously assigned from the data presented. This has recently been accomplished for the chicken liver enzyme from a comparison of the pH dependence of the kinetic parameters in both reaction directions (Nuiry & Cook, 1985). In the present studies however, enough information is available in the direction of oxidative decarboxylation to make the assignment. As stated above, the pH dependence of oxalacetate decarboxylation and pyruvate reduction catalyzed by NAD–malic enzyme has been obtained (Park, 1985). In both cases, the requirement is for a group with a pK of 5.6–6.0 to be protonated in order to hydrogen bond to the 2-keto group in both reactions. Thus, the group with a pK of 5.6 in E–Mg–malate and 4.8 in E–Mg–NAD must be unprotonated to accept a proton to form oxalacetate in the first portion of the reaction. This automatically fixes the protonation state of the group with a pK of 9 as being protonated.

Recent results from the pH dependence of the rate of inactivation by diethyl pyrocarbonate indicate that the group with a pK of 9 is a histidine (Rao et al., 1985a). Although this pK is somewhat high for an imidazole, it is certainly not

unprecedented. A pK value of ca. 9.5 is observed in similar studies of liver alcohol dehydrogenase (Hennecke & Plapp, 1983). In addition, the pH dependence of the rate of inactivation by butanedione (Rao et al., 1985b) suggests the presence of an arginine residue with a pK greater than 10 that is probably involved in malate binding.

The pH dependence of the K_i for inhibitors competitive against malate allows placement of the two groups with malate bound. The group with a pK of 4.9 in E–Mg–NAD must be hydrogen-bonded to the 2-hydroxyl group or, when protonated, hydrogen-bonded to the second carboxyl of oxalate (the first is presumably hydrogen-bonded to arginine). The group with a pK of 9 must be near the 3- and 4-carbons of malate since it is observed in the V/K_{malate} and tartronate pK_i profiles but not in the oxalate pK_i profile. Thus, this group can hydrogen bond to the 3- and 4-carboxyl groups of tartronate and malate, respectively, but not the 2-carboxyl of oxalate. The inhibitors effectively act as an active site titrant for the position of the general-acid catalyst.

The role of the metal is somewhat speculative but is given its normal role as a Lewis acid in the mechanism pictured in Figure 6 rather than adhering to previously suggested roles for the metal as an acid–base catalyst (Hsu et al., 1976; Schimerlik & Cleland, 1977b). This is a particularly attractive role for the metal, since oxalacetate is the intermediate generated upon decarboxylation of malate. Divalent metals are known to catalyze the decarboxylation of oxalacetate in solution (Westheimer & Jones, 1941; Westheimer, 1963).[6]

Thus, the group with a pK of 5.6 in E or E–Mg–malate and 4.8 in E–Mg–NAD abstracts the proton from the hydroxyl group at the 2-position of malate concomitant with hydride transfer [Figure 6 (I)] to produce the intermediate oxalacetate and NADH [Figure 6 (II)]. In agreement with oxalacetate as an intermediate, NAD–malic enzyme catalyzes the metal-dependent decarboxylation of oxalacetate (Park, 1985). The metal then acts as a Lewis acid (flow of electrons is toward the keto group coordinated to metal) to facilitate decarboxylation and also stabilize the resulting enolate anion [Figure 6 (III)]. The second base, probably a histidine residue (Rao et al., 1985a), in close proximity to the 3-position of the substrate as suggested by titration of the active site with substrate and inhibitors, must be protonated (pK of 9) and donates its proton to the enolate anion [Figure 6 (III)] to form pyruvate [Figure 6 (IV)].

Although the chemistry of the NAD–malic enzyme reaction and that of the NADP–malic enzyme reaction are probably similiar, the two enzymes are quite different kinetically. As already stated above, the kinetic mechanisms for the two enzymes are distinct, with an ordered mechanism for the NADP enzyme and a random mechanism for the NAD enzyme. From these studies, one also observes a distinct difference in the protonation mechanism for these two enzymes. The NADP enzyme will bind malate to both the correctly and incorrectly protonated enzyme forms but not equally well since there is a difference of 1.5 pH units in the pK values observed in the V and V/K_{malate} profiles (Schimerlik & Cleland, 1977b). On the other hand, the NAD enzyme has a strict requirement for binding of reactants to enzyme only when both acid–base catalysts are in their correct protonation states. In addition, the release of reduced nucleotide limits the overall reaction for the NADP enzyme except when catalysis becomes limiting at the pH extremes, while for the NAD enzyme, release of the reduced nucleotide is only a minor rate-limiting step until the pH is decreased to 4 where it becomes solely rate-limiting.

Malate is not very sticky in the NADP enzyme reaction but has a finite stickiness in the NAD enzyme reaction even though reactants appear to bind much more loosely to the NAD enzyme. Also, the pK values for the acid–base catalysts are observed at 6 and 8 in the V/K_{malate} profile for the NADP enzyme while the NAD enzyme displays pK values in the V/K_{malate} profile of 5 and 9, giving it a much broader pH optimum under all reaction conditions.

Finally, since NADPH release for the pigeon liver enzyme is 25 times slower than catalysis as opposed to only 2-fold for the ascarid enzyme, oxalate inhibition for the pigeon liver enzyme is predicted to be noncompetitive over the pH range 4–10. Therefore, both the pK_{is} and pK_{ii} profiles should decrease from a constant value at low pH to another constant value at high pH since over the entire pH range there is a significant amount of E–NADPH in the steady state to which oxalate can bind.

Registry No. NAD, 53-84-9; thio-NAD, 4090-29-3; NAD–malic enzyme, 9080-52-8; Mg, 7439-95-4; D_2, 7782-39-0; Cd, 7440-43-9; Mn, 7439-96-5; tartronic acid, 80-69-3; oxalic acid, 144-62-7; malic acid, 6915-15-7.

References

Allen, B. L., & Harris, B. G. (1981) *Mol. Biochem. Parasitol. 2*, 367.

Cleland, W. W. (1975) *Biochemistry 14*, 3220.

Cleland, W. W. (1977) *Adv. Enzymol. Relat. Areas Mol. Biol. 45*, 273.

Cleland, W. W. (1979) *Methods Enzymol. 63*, 103.

Cleland, W. W. (1982) *CRC Crit. Rev. Biochem. 13*, 385.

Cook, P. F., & Cleland, W. W. (1981a) *Biochemistry 20*, 1790.

Cook, P. F., & Cleland, W. W. (1981b) *Biochemistry 20*, 1797.

Cook, P. F., & Cleland, W. W. (1981c) *Biochemistry 20*, 1805.

Cook, P. F., Blanchard, J. S., & Cleland, W. W. (1980) *Biochemistry 19*, 4853.

Dawson, R. M. C., Elliot, W. H., & Jones, K. M., Eds. (1969) *Data for Biochemical Research*, p 208, 2nd ed., Oxford University Press, London.

Good, N. E., Winget, G. D., Winter, W., Connolly, T. N., Izawa, S., & Singh, R. M. M. (1966) *Biochemistry 5*, 467.

Hennecke, M., & Plapp, B. V. (1983) *Biochemistry 22*, 3721.

Hermes, J. D., Morrical, S. W., O'Leary, M. H., & Cleland, W. W. (1984) *Biochemistry 23*, 5479.

Hsu, R. Y. (1982) *Mol. Cell. Biochem. 43*, 3.

Hsu, R. Y., & Lardy, H. A. (1967) *J. Biol. Chem. 242*, 527.

Hsu, R. Y., Mildvain, A. S., Chang, G. Z.-G., & Fung, F. H. (1976) *J. Biol. Chem. 251*, 6574.

Landsperger, W. J., Fodge, D. W., & Harris, B. G. (1978) *J. Biol. Chem. 253*, 1868.

Martell, A. E., & Smith, R. M. (1979) *Critical Stability Constants*, Vol. 3, Plenum Press, New York.

Nuiry, I. I., & Cook, P. F. (1985) *Biochim. Biophys. Acta 829*, 295.

Park, S. H. (1985) Master's Thesis, North Texas State University, Denton, TX.

Park, S. H., Kiick, D. M., Harris, B. G., & Cook, P. F. (1984) *Biochemistry 23*, 5446.

[6] Recent work by Dr. George Reed at the University of Pennsylvania using EPR of E–VO^{2+} and E–VO–Ox (E is NAD–malic enzyme) complexes indicates that the latter complex is essentially identical with that found with pyruvate kinase. Dr. Reed has already shown that metal coordinates to the 2-keto and 1-carboxyl groups of pyruvate kinase reaction (personal communication). Thus, this also is most likely the case for NAD–malic enzyme.

Rao, J. G. S., Harris, B. G., & Cook, P. F. (1985a) *Arch. Biochem. Biophys. 241*, 67.
Rao, J. G. S., Harris, B. G., & Cook, P. F. (1985b) *Arch. Biochem. Biophys.* (submitted for publication).
Rose, I. A., O'Connell, E. L., Litwin, S., & Bar-Tana, J. (1974) *J. Biol. Chem. 249*, 5163.
Scharschmidt, M., Fisher, M. A., & Cleland, W. W. (1984) *Biochemistry 23*, 5471.
Schimerlik, M. I., & Cleland, W. W. (1977a) *Biochemistry 16*, 565.
Schimerlik, M. I., & Cleland, W. W. (1977b) *Biochemistry 16*, 576.
Uhr, M. L., Thompson, V. W., & Cleland, W. W. (1974) *J. Biol. Chem. 249*, 2920.
Viola, R. E., & Cleland, W. W. (1982) *Methods Enzymol. 87*, 353.
Viola, R. E., Cook, P. F., & Cleland, W. W. (1979) *Anal. Biochem. 96*, 334.
Westheimer, F. H. (1963) *Proc. Chem. Soc., London*, 253.
Westheimer, F. H., & Jones, W. A. (1941) *J. Am. Chem. Soc. 63*, 3283.
Yonetani, T., & Theorell, H. (1964) *Arch. Biochem. Biophys. 106*, 243.

Kinetics of Rapid Ca^{2+} Release by Sarcoplasmic Reticulum. Effects of Ca^{2+}, Mg^{2+}, and Adenine Nucleotides†

Gerhard Meissner,* Edward Darling, and Julia Eveleth

Departments of Biochemistry and Nutrition and of Physiology, School of Medicine, The University of North Carolina at Chapel Hill, Chapel Hill, North Carolina 27514

Received May 14, 1985

ABSTRACT: A radioisotope flux–rapid-quench–Millipore filtration method is described for determining the effects of Ca^{2+}, adenine nucleotides, and Mg^{2+} on the Ca^{2+} release behavior of "heavy" sarcoplasmic reticulum (SR) vesicles. Rapid $^{45}Ca^{2+}$ efflux from passively loaded vesicles was blocked by the addition of Mg^{2+} and ruthenium red. At pH 7 and 10^{-9} M Ca^{2+}, vesicles released $^{45}Ca^{2+}$ with a low rate ($k = 0.1$ s^{-1}). An increase in external Ca^{2+} concentration to 4 μM or the addition of 5 mM ATP or the ATP analogue adenosine 5′-(β,γ-methylenetriphosphate) (AMP-PCP) resulted in intermediate $^{45}Ca^{2+}$ release rates. The maximal release rate was observed in media containing 4 μM Ca^{2+} and 5 mM AMP-PCP and had a first-order rate constant of 30–100 s^{-1}. Mg^{2+} partially inhibited Ca^{2+}- and nucleotide-induced $^{45}Ca^{2+}$ efflux. In the absence of AMP-PCP, $^{45}Ca^{2+}$ release was fully inhibited at 5 mM Mg^{2+} or 5 mM Ca^{2+}. The composition of the release media was systematically varied, and the flux data were expressed in the form of Hill equations. The apparent n values of activation of Ca^{2+} release by ATP and AMP-PCP were 1.6–1.9. The Hill coefficient of Ca^{2+} activation ($n = 0.8$–2.1) was dependent on nucleotide and Mg^{2+} concentrations, whereas the one of Mg^{2+} inhibition ($n = 1.1$–1.6) varied with external Ca^{2+} concentration. These results suggest that heavy SR vesicles contain a "Ca^{2+} release channel" which is capable of conducting Ca^{2+} at rates comparable with those found in intact muscle. Ca^{2+}, AMP-PCP (ATP), and Mg^{2+} appear to act at noninteracting or interacting sites of the channel.

Sarcoplasmic reticulum (SR)[1] forms a distinct intracellular membrane compartment that regulates the contraction–relaxation cycle of muscle by releasing and reabsorbing Ca^{2+} [for reviews, see Ebashi (1976), Endo (1977), Winegrad (1982), Martonosi & Beeler (1983), and Inesi (1985)]. Release of Ca^{2+} from SR is triggered by an action potential at the neuromuscular junction that is communicated to SR via the T system. The mechanism by which Ca^{2+} is released from SR, however, has remained unclear. Mechanisms proposed to explain physiological release of Ca^{2+} include induction by Ca^{2+}, "depolarization" of the SR membrane, a change in membrane surface charge, and/or a pH gradient (Ebashi, 1976; Endo, 1977; Winegrad, 1982).

Of particular relevance to this study is the Ca^{2+}-induced Ca^{2+} release hypothesis which states that a small amount of Ca^{2+} moving into the sarcoplasm during an action potential induces the release of sufficient Ca^{2+} from SR to activate muscle contraction. In support of this hypothesis, skinned muscle fibers (Stephenson, 1981; Fabiato, 1983) and "heavy" SR vesicles obtained by centrifugation between 2000g and 10000g (Onishi, 1981; Yamamoto & Kasai, 1982; Miyamoto & Racker, 1982; Kirino et al., 1983; Morii & Tonomura, 1983; Nagasaki & Kasai, 1983; Kim et al., 1983; Meissner, 1984) possess a Ca^{2+} permeability mechanism which is activated by micromolar concentrations of Ca^{2+}. Caffeine and adenine nucleotides (ATP, ADP, AMP, adenosine, adenine) potentiated Ca^{2+}-induced Ca^{2+} release, whereas Mg^{2+} was inhibitory.

In this report, we describe a radioisotope flux–rapid-quench–Millipore filtration technique to determine the effects of Ca^{2+}, adenine nucleotides, and Mg^{2+} on the Ca^{2+} release

†Supported by U.S. Public Health Service Grant AM18687.
* Correspondence should be addressed to this author at the Department of Biochemistry and Nutrition, The University of North Carolina at Chapel Hill.

[1] Abbreviations: SR, sarcoplasmic reticulum; EGTA, ethylene glycol bis(β-aminoethyl ether)-*N,N,N′,N′*-tetraacetic acid; AMP-PCP, adenosine 5′-(β,γ-methylenetriphosphate); Pipes, 1,4-piperazinediethanesulfonic acid.

0006-2960/86/0425-0236$01.50/0